Measuring depth of anaesthesia using changes in directional connectivity: a comparison with auditory middle latency and estimated bispectral index during propofol anaesthesia -Supplementary Material

Methods

1. *Experimental Protocol*

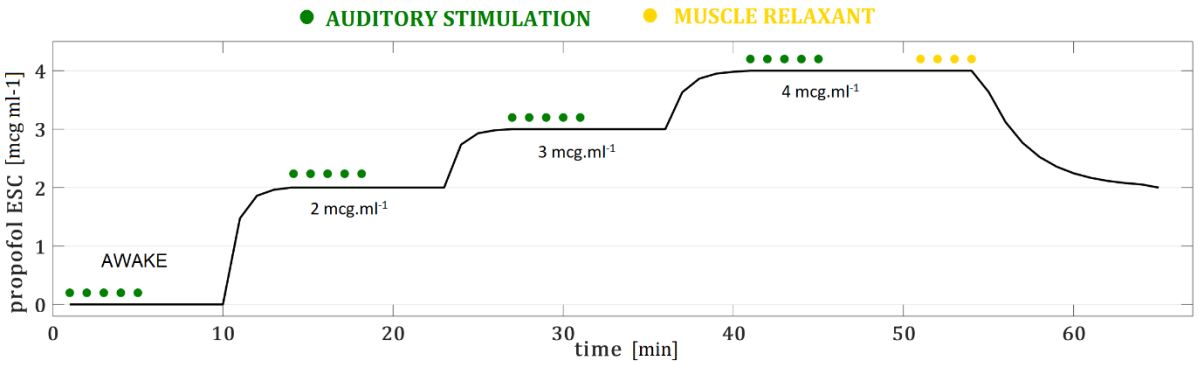

Figure S1. Experimental protocol schema: Target controlled infusion of propofol. Each point represents a 60 s epoch. The epochs in wakefulness (AWAKE) correspond to effect site concentration=0. The epochs where auditory stimulation was delivered are indicated on the effect site concentration time-line by green markers. Yellow markers indicate administration of muscle relaxant and tracheal intubation. Abbreviations: ESC: effect site concentration.

2. *Middle latency response estimation*

middle latency response were evoked using maximum length sequence as they have been showed to significantly increase the SNR as compared to traditional stimuli [1]. We used a maximum length sequences of order 4 with 8 stimuli in a sequence, repeated every 105 ms. The shortest allowable inter-stimulus interval in the sequence was 7 ms, giving a maximum stimulation rate of 143 Hz. The middle latency response is usually recorded placing the active electrode either on the midline forehead (Fz) or on the vertex (Cz), with the ground electrode on the low forehead. The position of the reference

electrode often represents an issue because of the myogenic interference of the postauricular muscle. Tooley and colleagues [2] showed that the vertex-inion electrode site gave the best results against the postauricular muscle artifact both in awake and anaesthetized subjects and reference electrode close to the nape of the neck are also recommended in [3]. In this study data were referenced with respect to the occipital electrode Oz and the channels Fz and Cz were selected for middle latency response estimation. Data were band pass filtered (15-250 Hz) and down-sampled to 1 kHz, as recommended by Bell and colleagues [3]. In order to remove the 50 Hz mains interference and its harmonics a bank of notch filters at 50, 150 and 250 Hz was also applied. All the filters were applied forwards and backwards in order not to introduce phase distortion. Data were then segmented in 105 ms epochs aligned with the stimulus onset and an amplitude threshold criterion (20 μV) was applied in order to remove artifactual trials. The number of epochs included in the estimation of middle latency response was then set to 2500 for all the experimental stages and subjects. In order to estimate the middle latency response evoked by a maximum length sequences sequence from the overlapped response a deconvolution algorithm [4] was additionally applied to the matrix of trials and then the coherent average performed. The SNR of the middle latency response was assessed using the F-value at a single point [5]. The F-value at a single point statistic is the ratio of the variance of the reconstructed middle latency response and the variance of the background noise (estimated as the variance of a single point at a fixed latency across trials). In this study we selected a latency of 30 ms from the stimulus onset for the single point and a time window of [30-80] ms to compute the power (variance) of the signal, according to the assumption that the brainstem response (up to 20 ms after the stimulus) is not affected by the level of arousal of the subject.

To determine if middle latency response responses were present in recordings that were significantly different from background noise, a bootstrap procedure was carried out for all the experimental stages and for each of the subjects. Each epoch of the original set of EEG data was de-trended and rotated starting at a random sample point (different for each epoch). For this bootstrap procedure, on

thousand epochs for each propofol effect site concentration were used. A `null middle latency response' estimate was obtained first applying the deconvolution algorithm and then the coherent average of the randomly rotated epochs. A F-value at a single point [5] for each of the bootstrap iterations was estimated as well. The same procedure was performed 500 times to obtain a null distribution for the middle latency response and the F-value at a single point value. The significance of the estimated middle latency response was assessed comparing the F-value at a single point value with the null F-value at a single point distribution obtaining, using the Davison and Hinkley (1997) formula, an empirical p-value. Before applying it to the study data, we have validated the bootstrap procedure assessing its false positive rate on white Gaussian noise. As a first step the middle latency response was computed using all the available non artifactual recordings for each experimental stage, i.e using 2500 sweeps, corresponding to 4.3 min of recordings for each propofol effect site concentration. This improves the quality of middle latency response estimation but on the other hand, due to the relatively long averaging period, may smear middle latency response changes in time and reduces the time resolution. In order to overcome these limitations and to allow comparison with other EEG indexes that were computed for 60 s segments, a second analysis was performed to obtain a time resolution of 1 min, therefore considering 600 epochs for the computation of the middle latency response.

3. BIS estimation

The BIS monitor has four electrodes placed on the forehead corresponding to the bipolar montage F3-F7 and Fz-F7 in the 10-20 international system [6], we therefore used electrodes F3 and Fz (with F7 as reference) to compute BIS. In order to reproduce as far as possible the proprietary algorithm for the computation of BIS [7,8], EEG signals were downsampled to 256 Hz, high pass filtered (0.5 Hz) and notch filtered with zero phase filters. The raw signals were divided in 2 s long segments and epochs with signals whose amplitude exceeded 100 μV were rejected. Due to the random nature of the EEG signals all the sub-parameters (beta ratio -β_R, burst suppression ratio -BSR and synchronization fast-

slow -SynchFS) [7] were computed for the 2 s epochs and then smoothed by averaging in 60 s segments (the BIS index value is therefore updated each minute). The BSR was computed as the fraction of epoch length in which the EEG was suppressed (|EEG| < 5 μV) for more than 0.5 s. The epochs were then preprocessed for frequency domain transformation by multiplication by a Blackman window. The spectral power was computed using direct FFT method and then averaging the complex product of FFT across 30 2 s long epochs; it was then integrated in empirical frequency bands to estimate the β_R, as indicated in the equation

$$\beta_R = log \frac{(Power)_{30-47\ Hz}}{(Power)_{40-47\ Hz}}$$

The bispectrum was computed using direct FFT method using the Matlab® function bispecd.m (1 Hz resolution, 75% of overlap) as in Miller et al.[8]. The SynFS parameter was then computed according to the equation:

$$SynchFS = log \frac{(Bispectral\ Power)_{0.5-47\ Hz}}{(Power)_{40-47\ Hz}}$$

Because of the symmetry properties of the bispectrum, the latter was computed only for the non-redundant subset of frequencies. As for the BSR, the β_R and the SynchFS were computed for each 2 s epoch and then averaged in 1 min long segments. The BIS proprietary algorithm combines the sub-parameters with weights extracted from a multivariate model based on a database of EEG recordings matched to corresponding hypnotic drug levels. The weights are assigned using a non-linear function and they vary depending on the anaesthetic stage: the β_R is dominant in light sedation, the SynFS during EEG activation and surgical level of hypnosis while the BSR detects deep anaesthesia. It has been shown that with increasing anaesthetic levels the BSR increases while the SynFS and β_R decrease [9]. In this analysis, we assessed the changes of the single sub-parameters and also combined them to obtain an estimated BIS index (eBIS). Considering that all the sub-parameters were reasonably on the same scale, we used the simple formula:

eBIS= -BSR +SynchFS + β_R

4. Connectivity estimation and validation

Directional connectivity was obtained from the multivariate (MVAR) model of multi-channel EEG time-series using directed coherence (DC) as reported also in our previous work [10,11]. DC quantifies the linear coupling from one channel to another as compared to all the other interactions with the signals of the multivariate dataset and it has been shown that the squared modulus of DCi,j(f) measures the normalized portion of the autospectrum of an EEG channel xi at frequency f due to the signal of channel j [14].

DC should be estimated from EEG epochs of adequate length to ensure that the number of samples is sufficient to accurately fit the model. Given an M-variate dataset, a minimum of M^2p data points is required for the model fitting (where M is the number of channels and p the MVAR model order), since there are M^2p parameters to estimate; however in practice a much higher number is recommended (i.e. $10M^2p$) for an accurate estimate [15]. In order to follow this recommendation and to reduce computational cost, which is always of concern in multivariate connectivity estimation, a reduced number of M=12 electrodes (Fp1, Fp2, F3, Fz, F4, C3, Cz, C4, P3, P4, O1, O2) and epochs of 60 s were considered for connectivity analysis.

It is crucial, when making inferences about EEG connectivity, to include in the analysis only statistically significant connections. In this study the significance of DC links was assessed by means of a surrogate data approach based on the phase shuffling of the EEG signals. EEG time series were phase shuffled in 1000 repetitions in order to generate a set of surrogate data in which any temporal correlation between channels was removed, but autocorrelation (and thus the spectrum) of each signal was preserved. DC was then estimated from the surrogate dataset and therefore an empirical null distribution for each pair of signals at all frequencies was obtained. The significance of causal links was assessed comparing the estimated connectivity with the null distribution, with a significance level at $p < 0.01$. Correction for multiple comparisons was performed using the false discovery rate

approximation for dependent measurements [16]. In addition to the statistical threshold, we applied thresholds to retain only the strongest connections. This procedure is widely recommended to discard weak (but significant) connections that may obscure the topology of strong links [17]. Since the choice of the threshold is somewhat arbitrary, results over a range of plausible thresholds (10%, 30% and 50% of strongest connections) were investigated.

Building on previous work [13,18], we focused the analysis on the dominant direction of information flow in the α band [8-13 Hz] [19–22] and long-range links [23,24], as these are most sensitive to changes in the level of consciousness. Since results in literature report that fronto-parietal connectivity undergoes critical changes with LOC [24–26], we assessed the number of statistically significant connections from centro-parietal (P3, P4, C3, C4, Cz), which we will call posterior, to frontal (Fp1, Fp2, F3, F4, Fz) electrodes and vice versa. In order to quantify the dominant direction of information flow on the fronto-posterior axis we defined an index ($Dir_{P\rightarrow A}$), given by the normalized differences of the number of links in the two opposite directions [27]. In order to summarize the individual DC features in a unique parameter for each subject and 60 s epoch e we summed the normalized strength of long-range links and the $Dir_{P\rightarrow A}$ to obtain what we have called the DCindex. The expression of the DCindex is given in equation 2). While the $Dir_{P\rightarrow A}$ (equation 1) is a normalized index varying from -1 to 1 for all the subjects[11], the strength of long-range DC can vary from one subject to another as a result of individual networks differences. For this reason we normalized the strength of DC links in each epoch by the average strength of long-range connectivity across all epochs in each subject.

$$Dir_{P\rightarrow A} = \frac{\sum_i \sum_j \left|DC\right|_{P\rightarrow A}^{\ 2} - \left|DC\right|_{A\rightarrow P}^{\ 2}}{\sum_i \sum_j \left|DC\right|_{P\rightarrow A}^{\ 2} + \left|DC\right|_{A\rightarrow P}^{\ 2}} \quad (1)$$

$$DCindex = \frac{\left|\overline{DC(e)}\right|^2}{\frac{1}{L}\sum_{e=1}^{L}\left|\overline{DC(e)}\right|^2} + Dir_{P\to A}(e), e = 1,..., L \quad (2)$$

In equation (2) $\left|\overline{DC(e)}\right|^2$ is the average strength (across electrode pairs) of connectivity links for the epoch *e* and *L* is the number of 60 s segments considered for each individual.

5. Wakefulness vs Anesthesia Classification

The aim of the study was to investigate the performances of the different EEG indexes in discriminating wakefulness from the different propofol effect size concentrations. To this end we used a binary classification procedure based on support vector machine [28]. A linear support vector machine classifier estimates the optimal linear combination of features (in this case middle latency response, BIS and DC sub-parameters) that separates the samples in distinct classes in the hyperspace of features. The optimal weights depend on the nature of the data and are usually found by training the support vector machine model on a number of datasets (also called 'folds') and then testing the model on the remaining data ('multi-folded cross-validation'). In this study we used a leave-one-out approach to cross-validate the support vector machine models: the model was trained on the entire set of observations except those relative to the specific subject, and then it was tested on the selected subject ('leave-one-out' procedure). The support vector machine was estimated by using a Sequential Minimal Optimization (SMO) routine [29]. The classifier's outputs are the probabilities of each observation (series of features) of belonging to a specific class. The posterior probability is estimated from the output scores of the classifier using a transform function [30].

We compared the performances of the EEG indexes using the linear support vector machine model with a non-linear classifier based on multilayer neural networks, to investigate if a more complex classifier would improve performances. neural network are mathematical models inspired to the

stimuli processing in the brain whose design include the choice of the activation function of the unit neurons, the particular learning algorithm and also the number of neurons in the hidden layer. We used the default Matlab® standard functions for pattern recognition (sigmoid function for the hidden layer, softmax for the output, conjugate gradient descent algorithm) which provide optimal performances. The number of neurons in the hidden layer is normally an undetermined parameter and has to be tested. We repeated the classification procedure for 2, 5, 10, 15, 20 and 25 neurons in the hidden layer, selecting the neural network with best performances as in [31].

Additional Results

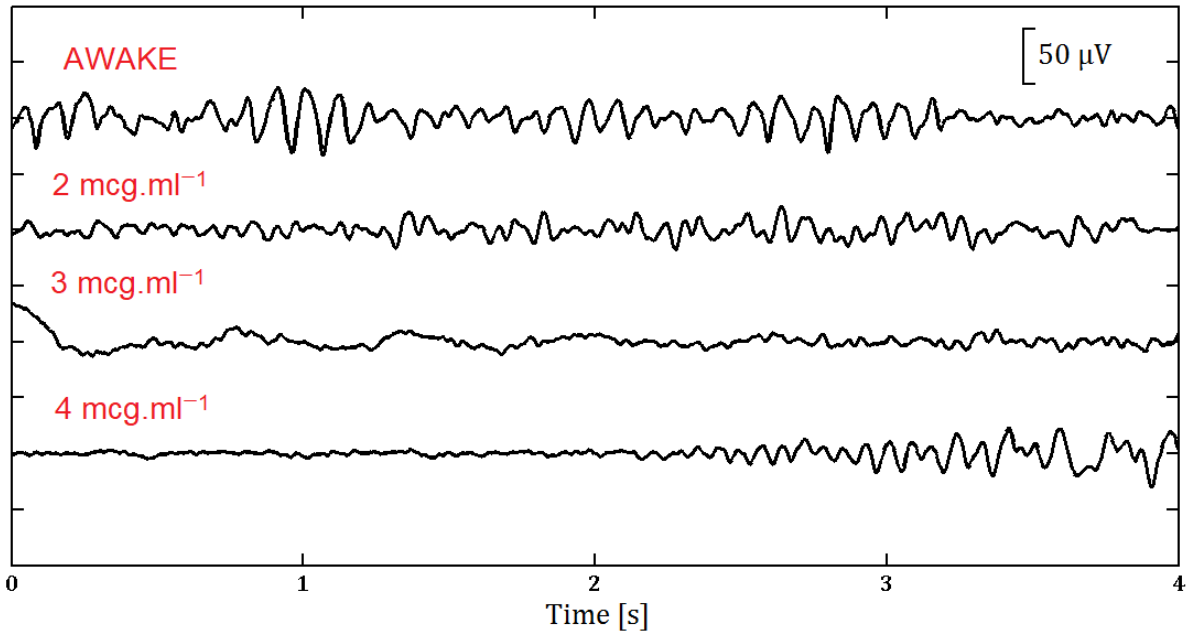

Figure S2. Representative examples of 4 s long EEG recordings in wakefulness and for increasing ESC levels in one subject (subject 1). Note the α (8-13 Hz) oscillation in wakefulness (first trace) and the increased β (13-30 Hz) activity for effect site concentration of 2 mcg.ml^{-1} *(second trace). For effect* site concentration of 3 mcg.ml^{-1} *the high amplitude slow waves are dominant (third trace) while deepest anaesthesia (*4 mcg.ml^{-1}*) is characterized by an alternation of burst (last second of the recording) and suppression (first three seconds) patterns.*

Connectivity

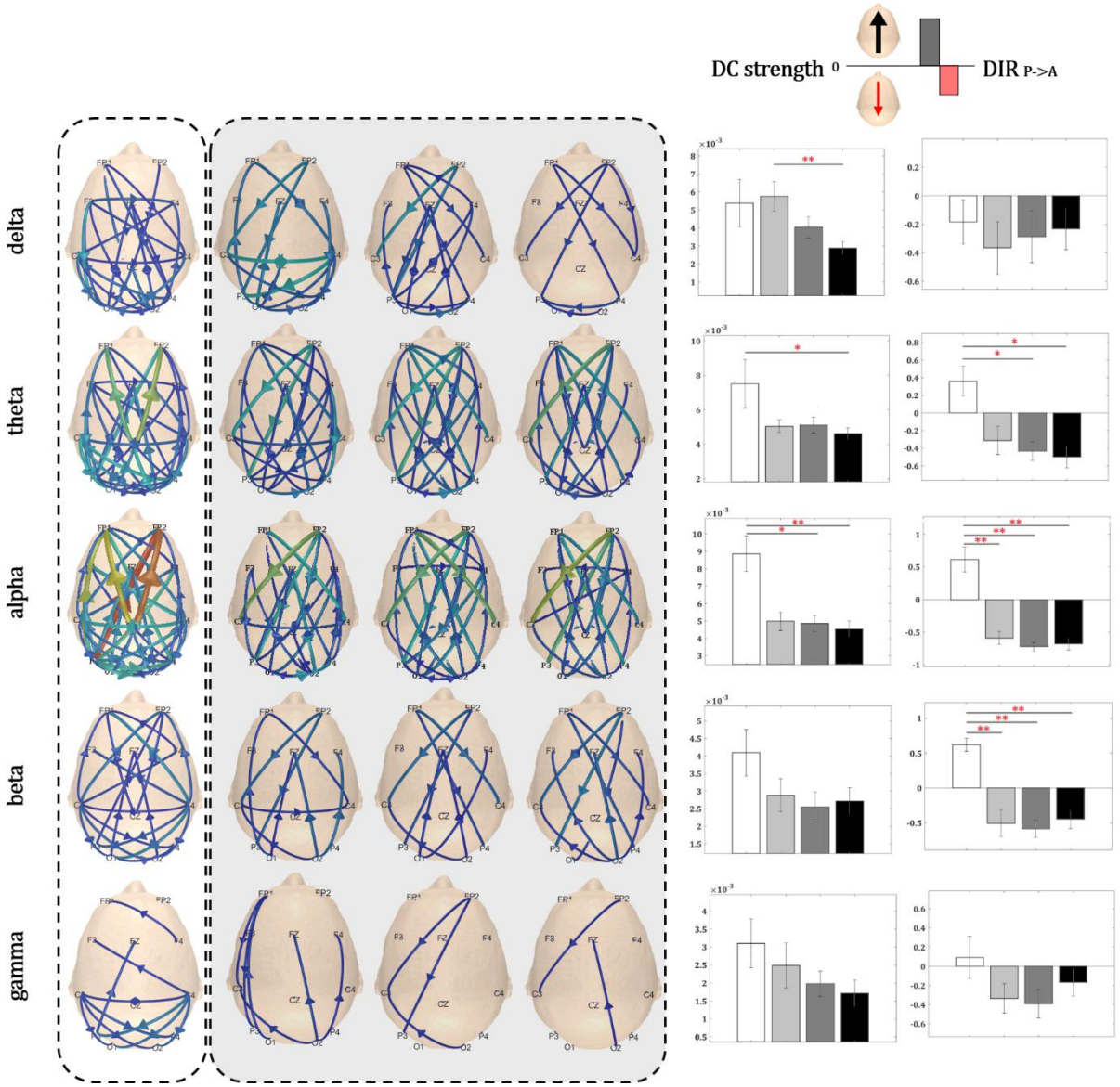

*Figure S3. Scalp topography of long-range connectivity networks, averaged across all 10 subjects, with associated statistics, plotted for five frequency bands of interest: delta [1-4 Hz], theta [4-8 Hz], alpha [8-13 Hz], beta [13-25 Hz], gamma [25-40 Hz] (30% strongest connections). Each subplot represents the Grand Average across subjects of long-range connections, with the color and size of arrows coding for the average strength of the specific link. The first column (white dashed box) refers to wakefulness, while plots of the last three column (gray dashed box) indicates results in anaesthesia (from left to right: effect site concentrations of 2 mcg.ml^{-1}, 3 mcg.ml^{-1} and 4 mcg.ml^{-1}). The bar plots on the right show the mean and standard error (across subjects) of the respective long-range links strength and $Dir_{P\rightarrow A}$ index during wakefulness (white), effect site concentrations of 2 mcg.ml^{-1}(light gray), 3 mcg.ml^{-1} (dark gray) and 4 mcg.ml^{-1}(black). *: $p < 0.05$; **: $p < 0.01$ (Friedman test). Based on these results,*

alpha was considered most sensitive to anaesthesia (which is also in accordance with expectations from the literature –[11,18]*) and used in the final index reported in the paper.* Abbreviations: DC: directed coherence.

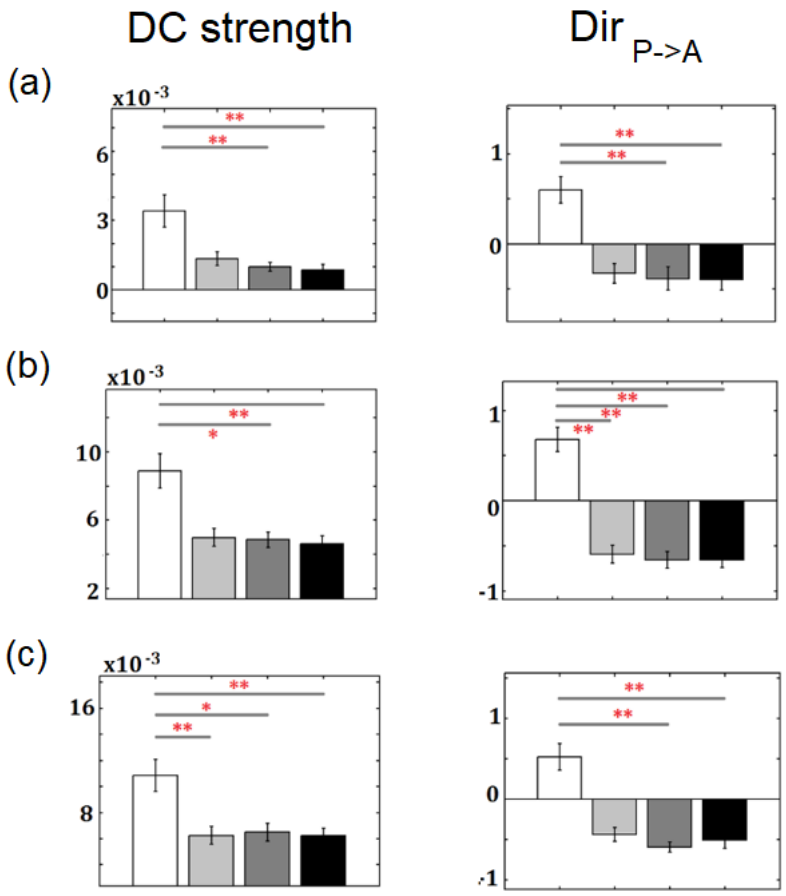

Figure S4. Mean and standard error (across subjects) of the strength of long-range directed coherence links and Dir $_{P\rightarrow A}$ for the 10% (a) 30% (b) and 50% (c) strongest connections (all connections shown are also statistically significant). Results during wakefulness (white), effect site concentration 2 mcg.ml^{-1}(light gray), effect site concentration 3 mcg.ml^{-1} (dark gray) and effect site concentration 4 mcg.ml^{-1}(black) are showed.;: p < 0.05; **: p < 0.01, Friedman and Tuckey's HSD tests.*

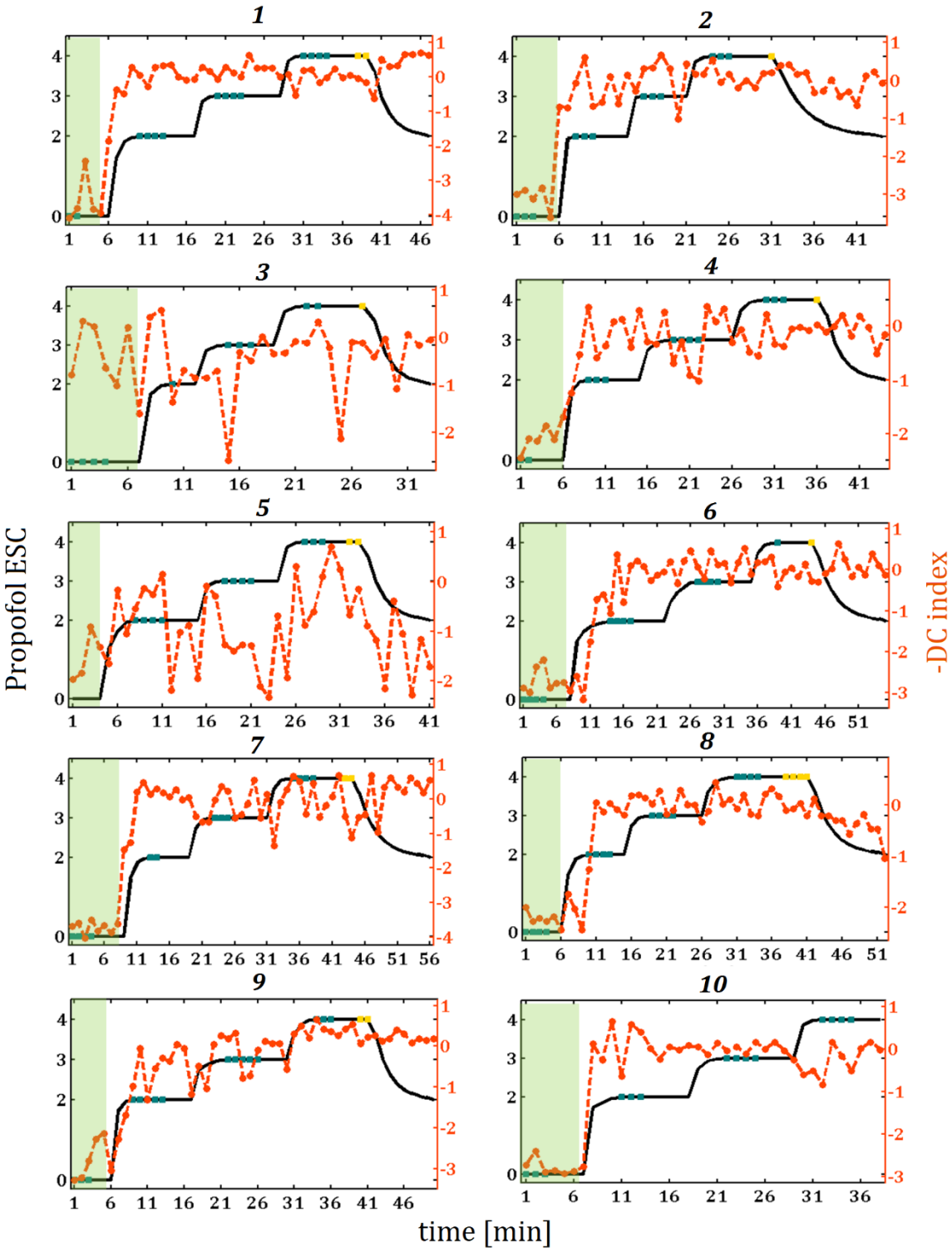

Figure S5. DCindex individual trends (dashed orange line) compared with effect site concentration time-line (black solid line) for the whole length of the recording and for all the subjects. The DCindex is inverted to facilitate comparison with the propofol effect site concentration. The epochs in wakefulness (effect site concentration=0) are highlighted in green and each time point refers to a 60 s epoch. The epochs where auditory stimulation was delivered are indicated on the effect site concentration time-

line by green markers while the epochs in which muscle relaxant was administered are indicated by yellow markers. In subject 10 the recovery period was heavily contaminated by artifacts and was excluded from the analysis. Abbreviation: ESC: effect site concentration.

1. *Middle latency response*

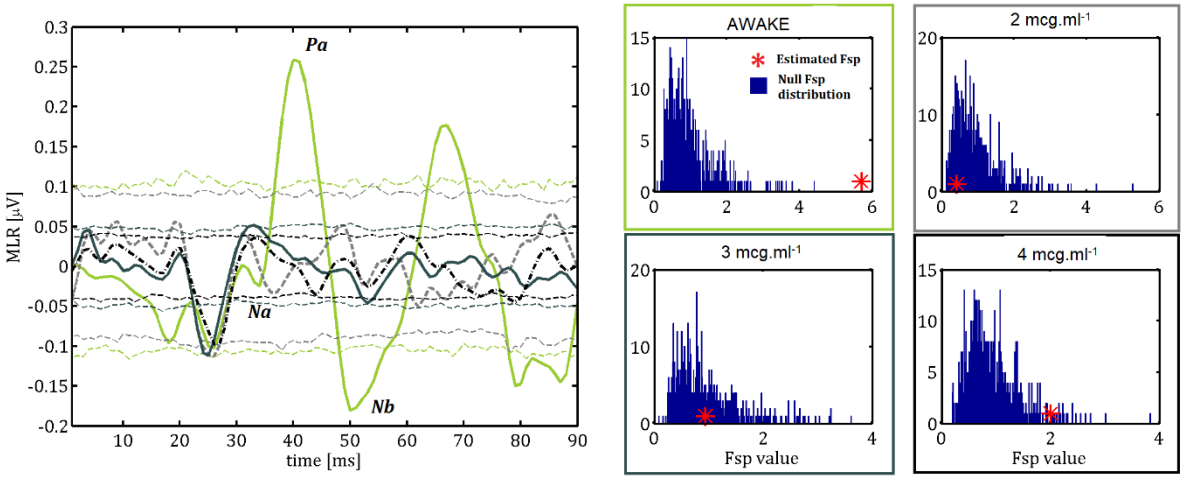

Figure S6. Representative example of middle latency response for increasing effect site concentrations (taken from subject 1). Left plot: middle latency response waveforms estimated from 2500 sweeps (4,3 minutes of recording) in AWAKE (green solid line),effect site concentration 2 mcg.ml^{-1} (light gray dashed line), effect site concentration 3 mcg.ml^{-1} (gray solid line), effect site concentration 4 mcg.ml^{-1} (black dashed-dotted line). The respective 95% critical values are showed in the same colours (thin dashed lines). Right Plot: Estimated F-value at a single point (red star) with relative null distribution (blue histogram) for each experimental stage. The empirical p-value obtained comparing the null distribution with the estimated F-value at a single point is indicated for each stage in the subplot title. Abbreviations: MLR: middle latency response; Fsp value: F-value at a single point.

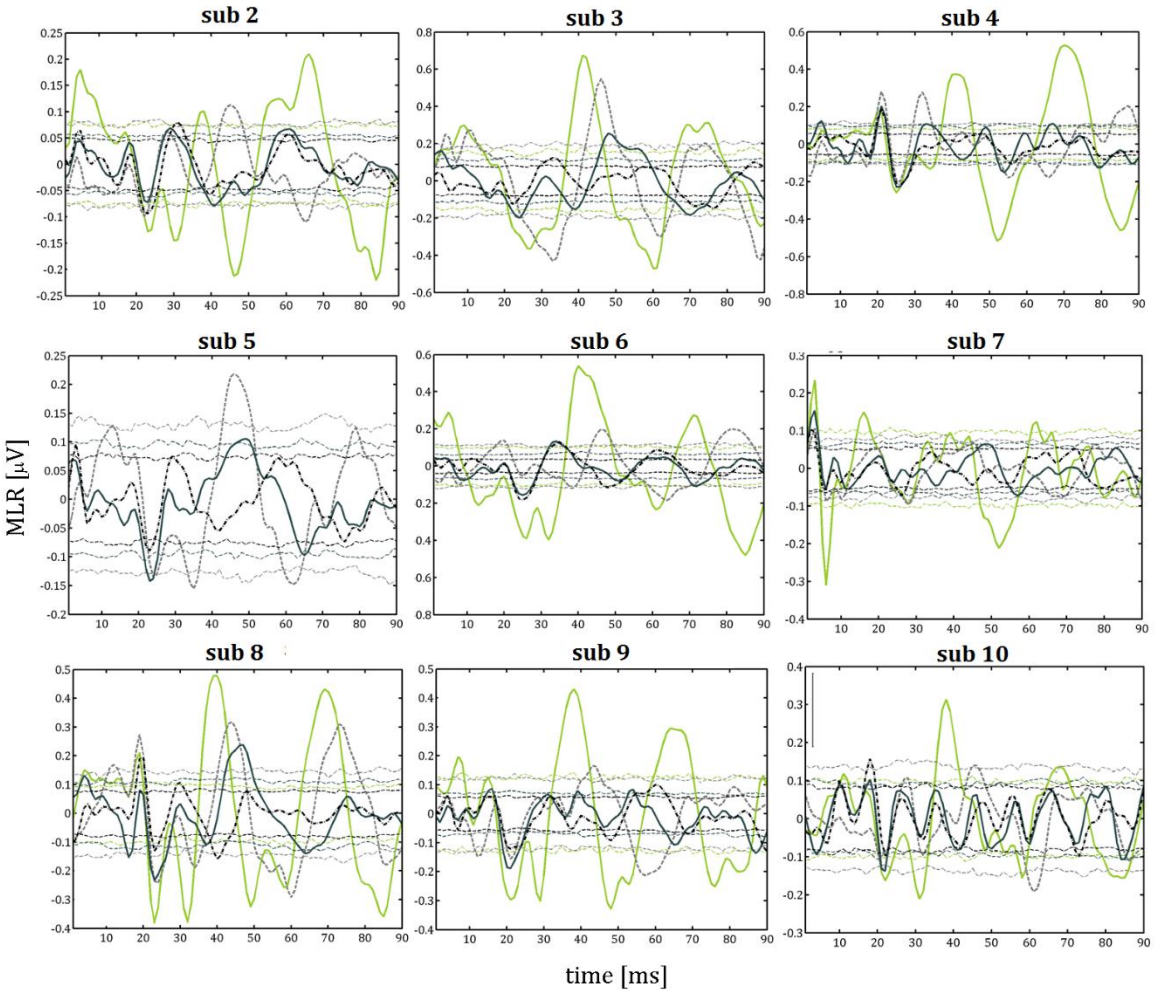

Figure S7. Middle latency response for increasing propofol effect site concentration in subjects 2 to 10. middle latency response waveforms were estimated from 2500 sweeps (4 minutes of recording) during wakefulness (green solid line), effect-site concentration of 2 mcg.ml^{-1} (light gray dashed line), effect-site concentration 3 mcg.ml^{-1} (gray solid line), effect-site concentration mcg.ml^{-1} (black dashed-dotted line). The respective 95% critical values are showed in the same colours. For some subjects the middle latency response exhibit an abrupt change during anaesthesia as observed in subject 1. However a more gradual effect was observed in other subjects (e.g. 3, 5, 8, 9) where the middle latency response amplitude more gradually decreases with the deepening of anaesthesia and a shift in the peaks latency is clearly identifiable. Abbreviations: MLR: middle latency response.

Subject	AWAKE	2 mcg.ml^{-1}	3 mcg.ml^{-1}	4 mcg.ml^{-1}
1	40	**NA**	**NA**	**NA**
2	36	55	69	67
3	50	52	60	66
4	42	45	44	46
5	**NA**	53	56	**NA**
6	51	54	62	69
7	42	**NA**	**NA**	**NA**
8	39	50	54	56
9	38	47	55	59
10	48	51	**NA**	**NA**
Mean $\pm$ Std	43.8 $\pm$ 5.4	50.8 $\pm$ 3.4	57.1 $\pm$ 7.7	60.5 $\pm$ 8.6

Table S1. Nb latency (ms) measured by visual inspection of the estimated middle latency response for all the subjects of the sample and experimental stages. The ***NA*** *symbol indicates the cases where it was not possible to objectively assess the Nb latency.*

2. *Awake vs Anaesthesia Classification*

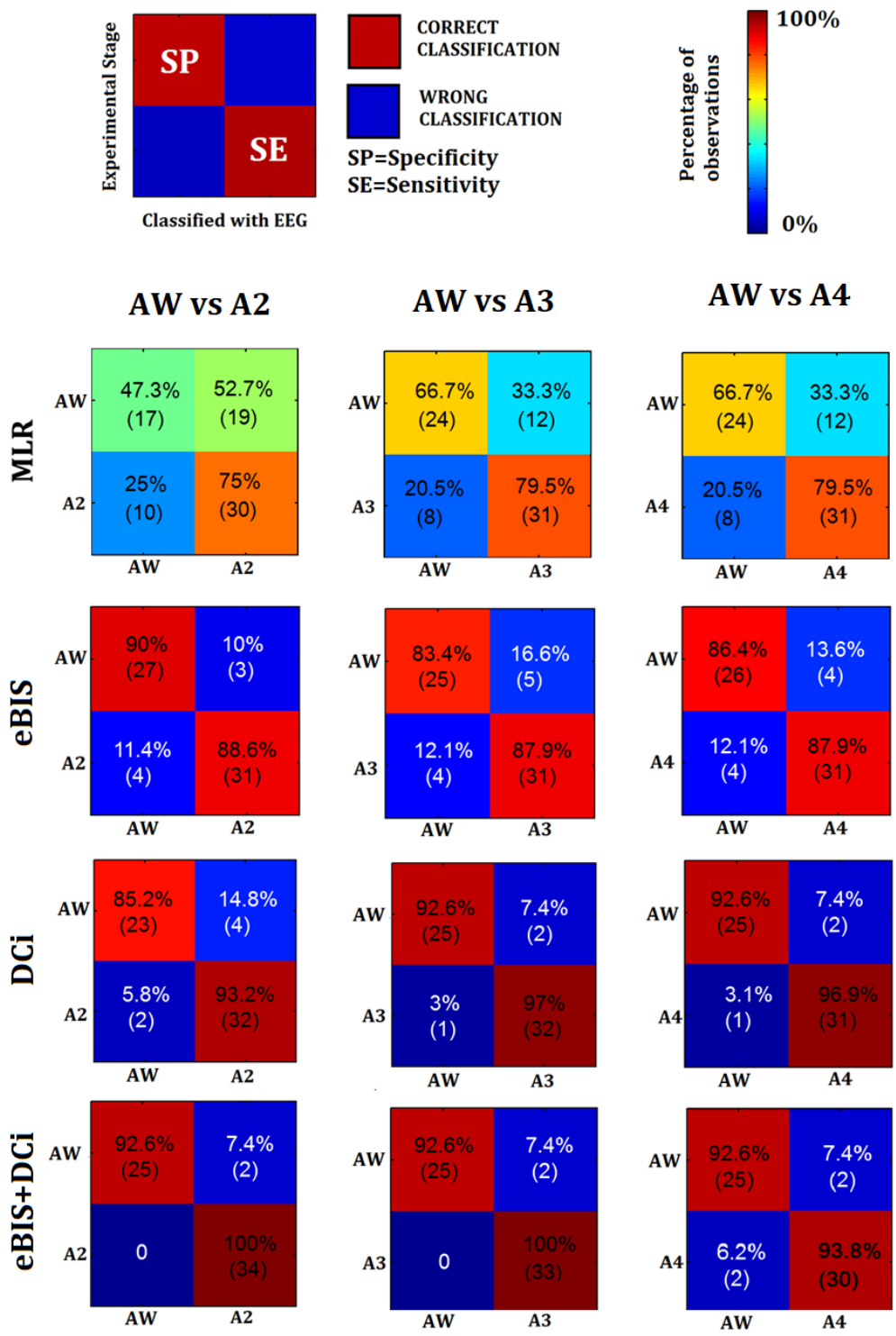

Figure S8. Comparison of support vector machine classification based on EEG indexes and experimental

stages assessed by propofol effect site concentration. The confusion matrices show on the y-axis the experimental stage and on the x-axis the prediction of the support vector machine classifier. The percentage of observations classified in each stage (and the associated number of observations in brackets) are reported in each cell. Elements on the main diagonal represent the percentage of correct classifications of `Awake' observations (Specificity, SP, first diagonal element) and `Anaesthesia' (Sensitivity, SE, second diagonal element), while on the opposite diagonal misclassifications are indicated. Different columns show results for the three binary classifications, while the rows refer to the type of EEG predictor used. Results for each of the different EEG indexes (middle latency response power, estimated BIS and DCindex, first three rows) and for the combination of DCindex and estimated BIS (last row) are showed. Abbreviations: MLR: middle latency response; eBIS: estimated BIS; DCi: DCindex; AW: wakefulness; A 2: effect site concentration of 2 mcg.ml^{-1}; A 3: effect site concentration of 3 mcg.ml^{-1}; A 4: effect site concentration of 4 mcg.ml^{-1}

	Accuracy			Specificity			Sensitivity		
	# TOT	SVM	NN	# AWAKE	SVM	NN	# ANES	SVM	NN
eBIS	131	0.901	0.90	30	0.767	0.716	101	0.95	0.941
DCi	126	0. 945	0.964	27	0.815	0.866	99	0.99	0.988
eBIS+DCi	126	0.966	0.964	27	0.889	0.833	99	0.99	1

Table S2. Average classification (`Awake' vs `Anaesthetized') performances (expressed as the fraction of correctly classified epochs) for the linear support vector machine classifier and the non-linear neural network classifier. For each performance descriptor (Accuracy, Specificity and Sensitivity) the number of epochs it was tested on is indicated: total number of epochs (#TOT) for the Accuracy, number of observations in wakefulness (#AWAKE) and anaesthesia (#ANES) for Specificity and Sensitivity, respectively. Results indicate results obtained with a linear support vector machine classifier are very similar to those relative to the non-linear neural network classifier. Abbreviations: DCi: DCindex; eBIS: estimated BIS; SVM: support vector machine (classifier); NN: neural network (classifier).

References

1. Bell SL, Smith DC, Allen R, Lutman ME. The auditory middle latency response, evoked using maximum length sequences and chirps, as an indicator of adequacy of anesthesia. *Anesthesia and*

analgesia 2006; **102**: 495–8.

2. Tooley MA, Stapleton CL, Greenslade GL, Prys-Roberts C. Mid-latency auditory evoked response during propofol and alfentanil anaesthesia. *British Journal of Anaesthesia* 2004; **92**: 25–32.

3. Bell SL, Smith DC, Allen R, Lutman ME. Recording the middle latency response of the auditory evoked potential as a measure of depth of anaesthesia. A technical note. *British journal of anaesthesia* 2004; **92**: 442–5.

4. Thornton ARD, Chambers JD, Folkard TJ. Deconvolution of MLS Response Data. 1998.

5. Erberling C, Don M. Quality Estimation Of Auditory Brainstem Responses. *Scandinavian audiology* 1984; **13**: 1887–197.

6. Johansen JW. Update on Bispectral Index monitoring. *Best Practice & Research Clinical Anaesthesiology* 2006; **20**: 81–99.

7. Rampil I. A Primer for EEG Signal Processing in Anesthesia The Genesis of the EEG Introduction-The Rationale for Monitoring. *Anesthesiology* 1998; **89**: 980–1002.

8. Miller A, Sleigh JW, Barnard J, Steyn-Ross DA. Does bispectral analysis of the electroencephalogram add anything but complexity? *British Journal of Anaesthesia* 2004; **92**: 8–13.

9. Morimoto Y, Hagihira S, Koizumi Y, Ishida K, Matsumoto M, Sakabe T. The relationship between bispectral index and electroencephalographic parameters during isoflurane anesthesia. *Anesthesia and analgesia* 2004; **98**: 1336–1340, table of contents.

10. Baccalá L a, Sameshima K. Partial directed coherence: a new concept in neural structure determination. *Biological cybernetics* 2001; **84**: 463–74.

11. Lioi G, Bell SL, Smith DC, Simpson DM. Directional connectivity in the EEG is able to discriminate wakefulness from NREM sleep. *Physiological Measurement* 2017; **38**.

12. Baccalá L a., Sameshima K, Ballester G, Do Valle a. C, Timo-Iaria C. Studying the Interaction Between Brain Structures via Directed Coherence and Granger Causality. *Applied Signal Processing* 1998; **5**: 40–8.

13. Lioi G, Bell SL, Smith DC, Simpson DM. Directional connectivity in the EEG is able to discriminate

wakefulness from NREM sleep. *Physiological Measurement* 2017; **38**: 1802–20.

14. Faes L, Nollo G. Multivariate Frequency Domain Analysis of Causal Interactions in Physiological Time Series. In: Mr Anthony Laskovski, ed. *Biomedical Engineering, Trends in Electronics, Communications and Software*. 2011th edn. INTECH Open Access Publisher, 2011.

15. Schlögl A, Supp G. Analyzing event-related EEG data with multivariate autoregressive parameters. *Prog Brain Res.* 2006; **159**: 135–47.

16. Benjamini Y, Yekutieli D. The control of the false discovery rate in multiple testing under depencency. *The Annals of Statistics* 2001; **29**: 1165–88.

17. Sporns O. Structure and function of complex brain networks. *Dialogues Clin Neurosci* 2013; **15**: 247–62.

18. Chennu S, Finoia P, Kamau E et al. Spectral Signatures of Reorganised Brain Networks in Disorders of Consciousness. *PLoS Computational Biology* 2014; **10**.

19. Purdon PL, Pierce ET, Mukamel EA et al. Electroencephalogram signatures of loss and recovery of consciousness from propofol. *Proceedings of the National Academy of Sciences of the United States of America* 2013; **110**: E1142-51.

20. De Gennaro L, Vecchio F, Ferrara M, Curcio G, Rossini PM, Babiloni C. Changes in fronto-posterior functional coupling at sleep onset in humans. *Journal of sleep research* 2004; **13**: 209–17.

21. Lee U, Kim S, Noh G-J, Choi B-M, Hwang E, Mashour G a. The directionality and functional organization of frontoparietal connectivity during consciousness and anesthesia in humans. *Consciousness and cognition* 2009; **18**: 1069–78.

22. Barrett AB, Murphy M, Bruno M-A et al. Granger causality analysis of steady-state electroencephalographic signals during propofol-induced anaesthesia. *PloS ONE* 2012; **7**: e29072.

23. Gómez F, Phillips C, Soddu A et al. Changes in effective connectivity by propofol sedation. *PloS one* 2013; **8**: e71370.

24. Ferrarelli F, Massimini M, Sarasso S et al. Breakdown in cortical effective connectivity during midazolam-induced loss of consciousness. *Proceedings of the National Academy of Sciences of the*

United States of America 2010; **107**: 2681–6.

25. Schrouff J, Perlbarg V, Boly M et al. Brain functional integration decreases during propofol-induced loss of consciousness. *NeuroImage* 2011; **57**: 198–205.

26. Boveroux P, Vanhaudenhuyse A, Bruno M-A et al. Breakdown of within- and between-network Resting State during Propofol-induced Loss of Consciousness. *Anesthesiology* 2010; **113**: 1038–53.

27. Lioi G, Bell SL, Simpson DM. Changes in functional brain connectivity in the transition from wakefulness to sleep in different EEG bands. *IFMBE Proceedings*. Vol57. 2016.

28. Brereton RG, Lloyd GR. Support vector machines for classification and regression. *The Analyst* 2010; **135**: 230–67.

29. Fan R, Chen P-H, Lin C. Working Set Selection Using Second Order Information for Training Support Vector Machines. *Journal of Machine Learning Research* 2005; **6**: 1889–918.

30. Platt JC. Probabilistic Outputs for Support Vector Machines and Comparisons to Regularized Likelihood Methods. *Advances in large margin classifiers* 1999; **10**: 61–174.

31. Nicolaou N, Georgiou J. Neural network-based classification of anesthesia/awareness using granger causality features. *Clinical EEG and Neuroscience* 2014; **45**: 77–88.